JPET Fast Forward. Published on December 2, 2022 as DOI: 10.1124/jpet.122.001407
This article has not been copyedited and formatted. The final version may differ from this version.

Protein 14-3-3 Influences the Response of the Cardiac Sodium Channel $Na_v1.5$ to Anti-Arrhythmic Drugs

Yang Zheng[1,2], Isabelle Deschênes[1]

1. Department of Physiology and Cell Biology, Frick Center for Heart Failure and Arrhythmias, Davis Heart and Lung Research Institute, The Ohio State University, Columbus, OH, USA

2. Department of Biomedical Engineering, Case Western Reserve University, Cleveland, OH, USA

JPET Fast Forward. Published on December 2, 2022 as DOI: 10.1124/jpet.122.001407
This article has not been copyedited and formatted. The final version may differ from this version.

Running title: 14-3-3 Influences $Na_v1.5$' Response to Anti-Arrhythmic Drugs

Corresponding Author: Isabelle Deschênes

Address: 333 W 10th Ave, Columbus, OH, 43210

Tel: (+1) 614-685-0614

Email: Isabelle.deschenes@osumc.edu

Number of text pages: 29

Number of tables: 1

Number of figures: 9

Number of references: 41

Number of words in the Abstract: 228

Number of words in the Introduction: 543

Number of words in the Discussion: 1685

List of abbreviations:

AADs: antiarrhythmic drugs; difo: difopein; ICD: implantable cardioverter-defibrillator; $Na_v1.5$: voltage-gated cardiac sodium channel; SCD: sudden cardiac death

Recommended section assignment:

Cardiovascular

JPET Fast Forward. Published on December 2, 2022 as DOI: 10.1124/jpet.122.001407
This article has not been copyedited and formatted. The final version may differ from this version.

Abstract

The cardiac sodium channel $Na_v1.5$ is a key contributor to the cardiac action potential and dysregulations in $Na_v1.5$ can lead to cardiac arrhythmias. $Na_v1.5$ is a target of numerous anti-arrhythmic drugs (AADs). Previous studies identified the protein 14-3-3 as a regulator of $Na_v1.5$ biophysical coupling. Inhibition of 14-3-3 can remove the $Na_v1.5$ functional coupling and has been shown to inhibit the dominant-negative effect of Brugada Syndrome mutations. However, it is unknown whether the coupling regulation is involved with AADs' modulation of $Na_v1.5$. Indeed, AADs could reveal important structural and functional information about $Na_v1.5$ coupling. Here we investigated the modulation of $Na_v1.5$ by four classical AADs, quinidine, lidocaine, mexiletine, and flecainide, in presence of 14-3-3 inhibition. The experiments were carried out by high-throughput patch-clamp experiments in an HEK293 $Na_v1.5$ stable cell line. We found that 14-3-3 inhibition can enhance acute block by quinidine, while the block by other drugs was not affected. We also saw changes in the use- and dose-dependency of quinidine, lidocaine, and mexiletine when inhibiting 14-3-3. Inhibiting 14-3-3 also shifted the channel activation toward hyperpolarized voltages in presence of the four drugs studied and slowed the recovery of inactivation in presence of quinidine. Our results demonstrated that the protein 14-3-3 and $Na_v1.5$ coupling could impact the effects of AADs. Therefore, 14-3-3 and $Na_v1.5$ coupling are new mechanisms to consider in the development of drugs targeting $Na_v1.5$.

JPET Fast Forward. Published on December 2, 2022 as DOI: 10.1124/jpet.122.001407
This article has not been copyedited and formatted. The final version may differ from this version.

Significance Statement

The cardiac sodium channel $Na_v1.5$ is a target of commonly used anti-arrhythmic drugs, and $Na_v1.5$ function is regulated by the protein 14-3-3. The present study demonstrated that the regulation of $Na_v1.5$ by 14-3-3 influences $Na_v1.5$'s response to anti-arrhythmic drugs. We provide detailed information about how 14-3-3 differentially regulated $Na_v1.5$ functions under the influence of different drug subtypes. Our findings will guide future molecular studies investigating $Na_v1.5$ and anti-arrhythmic drugs outcomes.

JPET Fast Forward. Published on December 2, 2022 as DOI: 10.1124/jpet.122.001407
This article has not been copyedited and formatted. The final version may differ from this version.

Introduction

Sudden cardiac death (SCD) associated with cardiac arrhythmia is the most common cause of death and remains a public health issue. SCD accounts for 15-20% of all death worldwide, and in the US alone, there are about 180,000-300,000 SCD cases annually. (Srinivasan and Schilling, 2018; Kim et al., 2021; Tan et al., 2021) Treatments for cardiac arrhythmias include cardiac ablation, implantable cardioverter-defibrillator (ICD), and anti-arrhythmic drugs (AADs). (Fu, 2015) AADs can treat cardiac arrhythmic conditions without surgical procedures and can be used as a preventive treatment. Therefore, AADs have great significance in clinical practice. Although the efficiency and safety of AADs have been tested by numerous experiments and clinical trials, not all aspects of the AADs' functions on their targets are fully understood, and the missing information can be essential in reducing side effects, improving efficacy, developing new drugs, and gaining knowledge of the target proteins.

The cardiac sodium channel $Na_v1.5$ is the predominant voltage-gated sodium channel in the human heart. It generates the cardiac sodium current (I_{Na}) that initiates the cardiac action potential, and dysregulation of I_{Na} can lead to arrhythmic phenotypes. (Fonseca and Vaz da Silva, 2018) $Na_v1.5$ is tightly regulated by interacting protein complexes. (Gavillet et al., 2006; Abriel, 2010) Dysfunction in $Na_v1.5$ regulatory proteins can also lead to cardiac arrhythmias. (Adsit et al., 2013; Xiong et al., 2022) As for many cardiac ion channels, $Na_v1.5$ is an essential target of AADs. AADs are categorized into five classes according to the Vaughan-Williams classification system. Class I AADs are sodium channel blockers. They block the sodium current to decrease the action potential's amplitude and slow conduction velocity, thus interrupting or preventing reentrant arrhythmias. (Pott et al., 2010) Considering that $Na_v1.5$ interacting proteins can

regulate the channel function, it is highly possible that certain $Na_v1.5$ regulatory proteins could affect the channel's response to AADs, thus influencing the AAD's outcome or side effects. However, there are limited studies that have investigated how the different $Na_v1.5$ regulatory proteins influence the action of AADs on $Na_v1.5$.

14-3-3 is one of $Na_v1.5$'s interacting proteins. It prevalently exists in all eukaryotic cells and regulates $Na_v1.5$'s function in the heart. (Allouis et al., 2006) Notably, other than the direct modulation of $Na_v1.5$ biophysical function, 14-3-3 was found to regulate $Na_v1.5$ coupling, a novel mechanism that can contribute to arrhythmic phenotypes. (Clatot et al., 2018; Zheng et al., 2021) Studies also suggested that modulating the action of 14-3-3 on $Na_v1.5$ could potentially bring therapeutic effects. This was also observed in other voltage-gated sodium channel isoforms related to neuronal disorders, therefore suggesting that 14-3-3 has a conserved role in regulating voltage-gated sodium channels. (Ruhlmann et al., 2020) However, the underlying mechanism of how 14-3-3 regulates $Na_v1.5$ coupling is not fully understood which limits its potential use as a therapeutic strategy. Additionally, it is unknown if the biophysical coupling regulated by 14-3-3 is involved in AADs action on $Na_v1.5$. Thus in this paper, we proposed to study the influence of protein 14-3-3 on Class I AADs' effects on the cardiac sodium channel. Cardiac sodium currents were studied by high-throughput automated patch-clamping using an HEK293 $Na_v1.5$ stable cell line. The specific 14-3-3 inhibitor difopein was used to determine if 14-3-3 and the sodium channel coupling impact the effects of AADs on $Na_v1.5$.

JPET Fast Forward. Published on December 2, 2022 as DOI: 10.1124/jpet.122.001407
This article has not been copyedited and formatted. The final version may differ from this version.

Materials and Methods

Materials

Quinidine (Q3625), flecainide (F6777), lidocaine (PHR1257), and mexiletine (M2727) were obtained from Sigma (St.Louis, MO). Drugs were diluted into a 100mM stock solution in water, methanol, or ethanol according to the manufacturer's instruction. Working concentrations of 20 (quinidine), 30 (flecainide), and 100μM (lidocaine and mexiletine) were freshly prepared in the electrophysiology extracellular solution.

Electroporation

The 14-3-3 inhibitor difopein (pEYFP-C1-difopein) (Clatot et al., 2017), (Masters and Fu, 2001) and negative control (pcDNA3.1) were transiently transfected into HEK293 cells by electroporation using ATx from MaxCyte (Gaithersburg, MD). HEK293 cells were plated 24 hours before electroporation and harvested on the day of electroporation at 70-80% confluency. Cells were collected by centrifugation at 1.1 rpm for 5min followed by washing with electroporation buffer (MaxCyte, Gaithersburg, MD). The cells were then resuspended to the concentration of 10^6 cells/μl, and mixed with the plasmid of interest at the concentration of 200ng/μl. The cells were electroporated and then incubated at 37°C for 20 min. Following incubation, the cells were transferred to 10cm dishes and grown for 48 h until patch-clamp experiments. Difopein expression level was confirmed before each patch-clamp experiment by observing the YFP signal under a fluorescent microscope.

Cell Culture and Expression of $Na_v1.5$

JPET Fast Forward. Published on December 2, 2022 as DOI: 10.1124/jpet.122.001407
This article has not been copyedited and formatted. The final version may differ from this version.

HEK293 $Na_v1.5$ stable cell line was maintained in DMEM (Gibco, Waltham, MA) supplemented with 10% FBS (Gibco, Waltham, MA) until used for transfection and electrophysiological recordings; 400 μg/ml G418 (Sigma, St.Louis, MO) was added to the medium for selection of $Na_v1.5$-HEK293 cells. All cells were grown at 37°C in 5% CO_2.

Electrophysiology Measurement

Sodium currents were measured by patch-clamping in the whole-cell configuration 48h after transfection. The recordings were obtained using the high-throughput automated patch clamp system Syncroptach 384i (Nanion, Germany). The patch-clamp experiments were conducted with high-throughput automated patch-clamp system Syncropatch 384i (Nanion, Germany). Compared with the traditional manual patch-clamp technology, the automated patch-clamp greatly increased the efficiency while eliminating operators' bias. The high number of cells being recorded all at the same time greatly reduced variability compared to manual patch-clamp and is particularly beneficial when studying pharmacological effects since it allows for all the cells to be exposed to the drugs for the exact same time. But most importantly, in our hands, the automated patch-clamp yield a highly consistent current profile compared with the manual patch-clamp in parallel (data not shown) illustrating that the data fully compare with manual patch-clamp. This observation is similar to the previous recordings of Nav1.7 channel with the high-throughput patch-clamp system previously reported. (Li et al., 2017) The intracellular solution contained (in mM):10 NaCl, 110 CsF, 10 CsCl, 10 EGTA, 10 HEPES, pH 7.4. The extracellular solution contained (in mM): 30 NaCl, 4 KCl, 2 $CaCl_2$, 1 $MgCl_2$, 5 glucose, 10 HEPES, 110 NMDG, pH7.4. Since sodium current density was high, low sodium concentration was used in the external solution and NMDG was used to balance the osmolarity. The current-

JPET Fast Forward. Published on December 2, 2022 as DOI: 10.1124/jpet.122.001407
This article has not been copyedited and formatted. The final version may differ from this version.

voltage relationships of the sodium currents were recorded by holding the resting membrane potential at -120mV and stepping from -80mV to +60mV in a 5mV interval (each step held for 30ms). For activation, the G/V curve was determined by fitting the linear part before the peak of the current-voltage curve with a Boltzmann function:

$$G(V) = G_{max}/(1 + e^{-(V-V_{half})/k})$$

Recovery from inactivation was recorded with a two-pulse protocol. The pre-pulse and the test-pulse duration are 30ms, stepping from -30mV to -120mV. The interval between the two pulses ranges from 1.8ms to 250ms. Currents of the recovery from inactivation were fitted to the following equation:

$$I_{test}/I_{pre-pulse} = A_{rec}(1 - \mathrm{e}^{-\mathrm{t}/\tau_{rec}}) + i_{rec}$$

The steady-state inactivation was studied with a 500ms pre-pulse ranging from -140mV to -30mV, followed by a 30ms test pulse stepping from -120mV to -30mV. The currents for the steady-state inactivation were fit to a Boltzmann distribution using the following equation:

$$I/I_{max} = (1 + e^{(V-V_{1/2})/k_v})^{-1}$$

The dose-dependency was studied with a single pulse from -120 to -10mV for 30ms. Cells harvested from the same dish were separated into different groups by the container of the automated patch-clamp system, the system then applied varied concentration of the drugs of interest to different groups and the sodium currents were recorded simultaneously from each group. I/V curves were recorded to confirm voltage control. Dose-dependency curves were fitted by the dose-response fitting with the following equation:

$$I/I_{max} = A1 + \frac{A2 - A1}{1 + 10^{(logx0-x)p}}$$

Use-dependency was studied with train pulses at 1, 5, and 10Hz. The holding potential was -120mV and the test pulses were -10mV. The use-dependency curves were fitted with an

JPET Fast Forward. Published on December 2, 2022 as DOI: 10.1124/jpet.122.001407
This article has not been copyedited and formatted. The final version may differ from this version.

exponential function. All fitting curves were generated with Origin 10.1.1 software (OriginLab Corporation, Northampton, MA). The leak subtraction protocol was used for all recording protocols. Cells with I_{Na} amplitude over 700pA/pF or with incomplete space-clamp were excluded from data analysis. (Montnach et al., 2021)

Statistical Analysis

Statistical analyses were performed using the standard statistical package in origin 10.1.1 (OriginLab Corporation, Northampton, MA). The student's t-test was performed at a significance level of p=0.05 for a single comparison. One-way ANOVA with post-hoc Tukey tests were performed for comparison among three or more groups, and p values less than 0.05 were considered statistically significant. Results were presented as mean ± SEM.

JPET Fast Forward. Published on December 2, 2022 as DOI: 10.1124/jpet.122.001407
This article has not been copyedited and formatted. The final version may differ from this version.

Results

Protein 14-3-3 is a family of highly conserved regulatory proteins. They were shown to bind with $Na_v1.5$ on the channel's intracellular loop and regulate $Na_v1.5$ function. 14-3-3 protein-protein interaction can be inhibited by a specific 14-3-3 inhibitor difopein (**di**meric **fo**urteen-three-three **pe**ptide **in**hibitor). As indicated by the name, difopein contains two repeats of the R18 peptide which occupied with high affinity the 14-3-3 groove supposed to bind to its target proteins. (Wang et al., 1999) The dimeric version of R18 (difopein) further improves the efficiency of 14-3-3-inhibitor binding, thereby disrupting 14-3-3 interacting with other proteins. (Stevers et al., 2018) Previous studies found that inhibiting 14-3-3 could remove the functional coupling of the voltage-gated sodium channel. (Clatot et al., 2017) Uncoupling the wildtype $Na_v1.5$ with Brugada Syndrome (BrS) mutations or splice variant associated with heart failure can restore the sodium current impaired by the mutation. (Clatot et al., 2018; Zheng et al., 2021) Thus, these previous findings suggested that 14-3-3 inhibitors could be a potential therapeutic strategy for arrhythmias linked to sodium channel dysfunction. However, since the molecular mechanism of the regulation of $Na_v1.5$ by 14-3-3 is still not completely understood and importantly, since 14-3-3 regulates the function of numerous proteins in the human body, additional investigations are needed in order to eventually develop therapeutic strategies targeting 14-3-3 for cardiac arrhythmias.

14-3-3 Inhibition Aggravated $Na_v1.5$ Block by Quinidine

In order to account for the impact of electroporation transfection effects, HEK293 cells transfected with 14-3-3 inhibitor difopein were compared with those transfected with pcDNA3.1. For simplicity, the groups transfected with control plasmid (pcDNA3.1) and recorded in the

JPET Fast Forward. Published on December 2, 2022 as DOI: 10.1124/jpet.122.001407
This article has not been copyedited and formatted. The final version may differ from this version.

absence of AADs were labeled 'control', the groups transfected with control plasmid and treated with the AAD were labeled by the AAD's name (i.e. 'quinidine'), and the groups transfected with difopein and treated with the AAD were labeled by the AAD's name_difo (i.e. 'quinidine_difo'). Cardiac sodium currents with and without 14-3-3 inhibition were recorded from HEK293 $Na_v1.5$ stable cell line in the presence of quinidine (class Ia), lidocaine (class Ib), mexiletine (class Ib), and flecainide (class Ic). The I/V curves were plotted to show the voltage-dependency in presence of AADs and 14-3-3 modulation. As expected, all four drugs blocked sodium currents. 14-3-3 inhibition and AADs' block did not change the current-voltage relationship of the sodium channel. However, 14-3-3 inhibition significantly aggravated the block by quinidine, while the current reductions for the other drugs remained unchanged in presence of 14-3-3 inhibition. Figure 1A shows representative examples of the sodium currents reduction caused by quinidine with and without 14-3-3 inhibition. The I/V relationships are illustrated in Figure 1B. The peak current was reduced from -233.14±18.96 pA/pF (n=36) to-185.10±13.66 pA/pF (n=33) in presence of quinidine in the control group and from -248.68±18.97 pA/pF (n=31) to -125.63±12.47 pA/pF (n=35) in the difopein (14-3-3 inhibitor) group. However, 14-3-3 inhibition did not modify the block in sodium currents by lidocaine, mexiletine, and flecainide (Figure 1C). I/V curves for lidocaine, mexiletine, and flecainide are shown in Supplemental Figure 1. We also obtained $Na_v1.5$ conductance curves from the current-voltage relationship. We found that when the AADS were applied in presence of 14-3-3 inhibition, all the activation curves were shifted toward hyperpolarizing voltages compared to the response to AADs alone (Figure 2). Interestingly, with 14-3-3 inhibitor difopein, the resulted G/V curves for lidocaine+difopein and mexiletine+difopein behave similarly to the control

JPET Fast Forward. Published on December 2, 2022 as DOI: 10.1124/jpet.122.001407
This article has not been copyedited and formatted. The final version may differ from this version.

groups in which the corresponding drugs were absent (Figure 2B-C). This suggests that 14-3-3 is involved in the regulation of the conductance by class Ib AADs.

14-3-3 Inhibition Altered $Na_v1.5$ Steady-State Inactivation and Recovery from Inactivation in Response to AADs

To elucidate the influence of 14-3-3 on AADs' effects on channel kinetics, we examined $Na_v1.5$ steady-state inactivation (SSI) and recovery from inactivation in presence of AADs with and without 14-3-3 inhibition. While quinidine shifted the channel SSI toward depolarized voltages, interestingly this shift was absent with 14-3-3 inhibition (Figure 3A). No change in SSI was observed when lidocaine and flecainide were applied; however, when the drugs were applied in presence of difopein, SSI was shifted toward hyperpolarized voltages (Figure 3B, 3D). For mexiletine, we saw no effect on SSI with or without difopein (Figure 3C). We then assessed recovery from inactivation. We found that both Class Ib AADs, lidocaine and mexiletine, induced a profound slowing in the recovery from inactivation; however, this slowing in the recovery was still present with 14-3-3 inhibition (Figure 4B-C) suggesting that 14-3-3 is not involved with this AADs effect on I_{Na}. In presence of quinidine, we did not see a change in the recovery from inactivation; however, when the drug was applied in presence of 14-3-3 inhibition, recovery from inactivation was slowed (Figure 4A). No obvious changes were seen in recovery from inactivation for flecainide with or without 14-3-3 inhibition. (Figure 4D) A summary of the biophysical parameters is shown in Table 1.

Impact of 14-3-3 on AADs' Dose-dependent Block

JPET Fast Forward. Published on December 2, 2022 as DOI: 10.1124/jpet.122.001407
This article has not been copyedited and formatted. The final version may differ from this version.

AADs' effects on $Na_v1.5$ depend on the concentration of drugs applied which is referred to as the dose-dependency of the inhibition. To study whether 14-3-3 affects the AADs' dose-dependent block, we recorded sodium currents at different drug concentrations with or without 14-3-3 inhibition. The normalized sodium currents were plotted and dose-dependency curves were generated by curve fitting. The results showed that 14-3-3 inhibition significantly changed the dose-dependency for quinidine, a class Ia anti-arrhythmic drug (Figure 5A). The calculated IC50s without and with 14-3-3 inhibition were 102.1 μM and 7.4 μM respectively. This suggests that a much smaller quinidine concentration is needed to have the same level of sodium currents block. On the other hand, 14-3-3 inhibition tended to move the dose-dependent curve of flecainide in the opposite direction (Figure 5D). The IC50s for flecainide were 84.3 μM and 141.3 μM with and without 14-3-3 inhibition respectively. For the Class Ib AADs, lidocaine and mexiletine, there were no obvious changes in the dose-dependency curves and the changes in IC50s were not statistically significant (Figure 5). The IC50 for lidocaine were 198.6 μM and 192.0 μM, and for mexiletine were 285.9 μM and 208.3 μM before and after 14-3-3 inhibition respectively.

14-3-3 Altered Use-dependency of $Na_v1.5$ on Lidocaine

The sodium currents blocked by a drug reflect the rate of binding and releasing of the drug to or from the sodium channel. This rate can be altered by high-frequency stimulation, known as a use-dependent or frequency-dependent block. All AADs (quinidine, lidocaine, mexiletine, and flecainide) studied in this paper are known to block $Na_v1.5$ in a use-dependent manner, meaning that the channel's availability would decrease progressively with a train of stimulation. (Hondeghem and Matsubara, 1988; Sunami et al., 1993; Zhu et al., 2006; Cummins, 2007) To

test whether 14-3-3 influences the use-dependent block by AADs, we applied depolarization trains to the channel with varied frequencies (1, 5, and 10 Hz). At 1Hz, which correlates with physiological heart rate, we applied 50 pulses and 30 pulses were applied for higher frequencies (5 and 10 Hz). All AADs exhibited use-dependent block with or without 14-3-3 inhibition (Figure 6-8). There was no significant effect of 14-3-3 inhibition on the use-dependency of quinidine at any tested frequency (Figure 9A). At 1Hz, 14-3-3 inhibition increased the use-dependent inhibition of the Class Ib drug lidocaine (Figures 6B and 9B). However, at higher frequencies, 14-3-3 inhibition significantly reduced the use-dependent block by lidocaine and mexiletine (Figures 7B-C, 8B-C, 9B-C). In the flecainide group, 14-3-3 inhibition had no effect on the use-dependent block at 1Hz (Figures 6D and 9D) but significantly attenuated the use-dependent block at 5Hz (Figures 7D and 9D). In summary, 14-3-3 inhibition changed the use-dependent block of lidocaine, mexiletine and flecainide, and exerted the most drastic effects at 5Hz suggesting the involvement of 14-3-3 in use-dependent blocks of Class Ib and Class Ic AADs.

Discussion

In this study, we examined the influence of protein 14-3-3 on the cardiac sodium channel's response to four commonly used antiarrhythmic drugs. These drugs are often applied as control compounds to study the sodium channel or novel pharmaceutical agents. (Hondeghem and Matsubara, 1988; Ramos and O'Leary M, 2004; Zhu et al., 2006; Cummins, 2007; Heath et al., 2011; Huang et al., 2013; Galleano et al., 2021; Li et al., 2021) Thus they were selected here to study the influence of 14-3-3 on $Na_v1.5$'s pharmaceutical response. Our results demonstrated that 14-3-3 could affect the pharmacological sensitivity of $Na_v1.5$ towards clinically used drugs,

JPET Fast Forward. Published on December 2, 2022 as DOI: 10.1124/jpet.122.001407
This article has not been copyedited and formatted. The final version may differ from this version.

providing further mechanistic insights into the action of anti-arrhythmic drugs on the cardiac sodium channel.

14-3-3's Effects on Quinidine Block

Quinidine is a Class Ia AAD known to block $Na_v1.5$ in a voltage- and use-dependent manner. In the current study, we found that inhibiting 14-3-3 brought a more potent block by quinidine of the peak sodium current. With 20μM quinidine, the peak sodium current was blocked by 21% in the control group and by 50% when 14-3-3 was inhibited. This result suggested that 14-3-3 inhibition might strengthen quinidine's effect on prolonging the cardiac action potential phase 0. (Salata and Wasserstrom, 1988) However, this enhancement is unlikely to be through modulation of the channel inactivation based on our observation that 14-3-3 inhibition removed the depolarizing shift caused by quinidine on SSI (Figure 3A). Recent structural studies found that quinidine binds with the channel in the channel lumen as well as a fenestration between Domain II (DII) and Domain III (DIII). (Li et al., 2021) Since the fenestration is likely to be reshaped during channel gating and the accompanying conformational changes, it is plausible that 14-3-3's interaction with $Na_v1.5$ would affect this fenestration, thus changing quinidine's accessibility. Interestingly, sodium channel mutations near the 14-3-3 binding sites were also shown to alter the channel's response to quinidine, (Itoh et al., 2005; Shuraih et al., 2007) further suggesting the possible involvement or influence of 14-3-3 in quinidine binding.

14-3-3's Influence on the Channel Activation

The protein 14-3-3 was first identified as a regulator of $Na_v1.5$ by yeast two-hybrid screening and functional studies in COS-7 cells. (Allouis et al., 2006) The study also showed that $Na_v1.5$

JPET Fast Forward. Published on December 2, 2022 as DOI: 10.1124/jpet.122.001407
This article has not been copyedited and formatted. The final version may differ from this version.

activation was not influenced by 14-3-3. (Allouis et al., 2006) Here in the present study, we focused on the impact of 14-3-3 on AADs' effects instead of the direct regulation of 14-3-3 on the channel. We found that 14-3-3 inhibition consistently shifted the channel's activation toward hyperpolarized voltages under the influence of all AADs studied. It is possible that the AADs' block could unmask the effects of 14-3-3 on channel activation. Alternatively, this might be explained by the fact that 14-3-3 might promote the channel activation under the influence of Class I blockers. The influence of 14-3-3 inhibition on $Na_v1.5$ activation in the presence of AADs' is reminiscent of our previous observation that $Na_v1.5$ coupling presumably took a role in the channel activation. (Clatot et al., 2017) The ubiquity of the 14-3-3 effects on channel activation under AADs' influences indicated that the channel coupling could impact channel activation. On the other hand, these results also suggest that $Na_v1.5$ coupling most likely alters the channel's pharmaceutical response.

Among the four tested AADs, we found that class Ib AADs lidocaine and mexiletine shifted the activation curves toward depolarized voltages. Interestingly, the curves were shifted back toward the control with 14-3-3 inhibition (Figure 2B-C). This indicated that while class Ib AADs could delay $Na_v1.5$ activation, protein 14-3-3 is necessary for this regulation.

Regulation of Use-Dependent Block by 14-3-3

The voltage-gated sodium channel's responses to high-frequency stimulation can be blocked more readily than responses to low-frequency, known as use-dependent blocking. This enhanced blocking potency during rapid stimulation can be explained by a varied equilibrium with the "reactivity" of the channel-drug interaction. (Starmer et al., 1984) Based on our finding that 14-3-3 inhibition increased the acute quinidine block of the peak sodium current, one might expect

JPET Fast Forward. Published on December 2, 2022 as DOI: 10.1124/jpet.122.001407
This article has not been copyedited and formatted. The final version may differ from this version.

to see effects of 14-3-3 inhibition on the quinidine's use-dependent block. However, use-dependent represents the accumulated effect of a drug during high-frequency repetitive stimulations. It reflects the rate of binding and release of the drug to and from the channel which might not require the modified channel kinetics. (Starmer et al., 1984) It is therefore feasible to observe a more potent block of peak current but no effect on use-dependency. Indeed, we observed that the use-dependent block by quinidine was not affected by 14-3-3 inhibition (Figure 9A).

We reported in this study that 14-3-3 inhibition significantly changed the use-dependent inhibition of class Ib AADs lidocaine and mexiletine. We observed that the use-dependent inhibition is not as significant for lidocaine and mexiletine at 1Hz compared to other drugs (Figure 6). This is consistent with previous findings and with the knowledge that class Ib AADs have relatively fast dissociation kinetics, thus being less affected by use-dependent block at low frequency. (Wang et al., 2015; Shenasa et al., 2020) Here in our study, the 14-3-3 inhibition had the tendency to increase the use-dependent block induced by lidocaine and mexiletine at 1Hz. However, 14-3-3 impacted the use-dependent block of these two drugs at 5 and 10 Hz impairing the use-dependent block (Figure 9). This indicates that 14-3-3 could regulate $Na_v1.5$ and its interaction with AADs differentially with increased heart rate. Importantly, the effects on use-dependent block and the 14-3-3 inhibition showed similar patterns for the two class Ib drugs but different patterns for class Ia and Ic AADs, suggesting that the 14-3-3 regulation is in line with the mode of action of varied AAD subclasses.

Different Impact of 14-3-3 Regulation on Different AAD Subtypes

JPET Fast Forward. Published on December 2, 2022 as DOI: 10.1124/jpet.122.001407
This article has not been copyedited and formatted. The final version may differ from this version.

In the dose-dependent block experiments, we observed that 14-3-3 inhibition significantly lowered the IC50 of quinidine, meaning that 14-3-3 increased $Na_v1.5$'s sensitivity towards quinidine. Meanwhile, there was little effect on the dose-dependence of other tested drugs. This is consistent with the other results shown by the I/V curve where 14-3-3 inhibition aggravated sodium current block by quinidine while the block by other drugs was not significantly changed (Figure 1). In our experiments, the IC50 of class Ic (flecainide), Ia (quinidine), and Ib (lidocaine and mexiletine) AADs were 84, 102, 198, and 286 μM respectively. These results reproduced the order of sodium channel block by these drugs in clinical practice and previous investigations, which was class Ic > Ia > Ib. (Kecskemeti, 1991)

We also found that the 14-3-3 inhibition did not influence the dose-dependence of the class Ib AADs lidocaine and mexiletine. As discussed earlier, we observed a similar pattern for 14-3-3 inhibition effects on activation and use-dependent block with the two class Ib AADs. The two class Ib AADs acted similarly in response to 14-3-3 inhibition throughout our study, and this is consistent with AADs' mode of action and the molecular interaction between the channel and the drugs. Previous investigations demonstrated that only class Ib AADs bind with the channel via a strong electrostatic cation-pi interaction, which could significantly influence the binding mode and affinity of a compound. (Ragsdale et al., 1996; Liu et al., 2003; Pless et al., 2011; Tikhonov and Zhorov, 2017) It is possible that this interaction also led to the differential response of class Ib AADs to 14-3-3 inhibition. This specific and similar impact of 14-3-3 inhibition on the action of the two class Ib drugs might also suggest that the electrostatic cation-pi interaction of the drugs with the channel is dependent on the biophysical coupling modulated by 14-3-3.

JPET Fast Forward. Published on December 2, 2022 as DOI: 10.1124/jpet.122.001407
This article has not been copyedited and formatted. The final version may differ from this version.

Structural and functional studies showed that the DIV S6 of $Na_v1.5$ is the key site for drug binding. (Ragsdale et al., 1994; Ragsdale et al., 1996) However, the $Na_v1.5$ dimerization, as well as the 14-3-3 regulation depend more on the DI-DII linker. (Allouis et al., 2006; Clatot et al., 2017) Although further investigations on the 3D structure are needed, the current understanding of the spatial relationship between the DI-DII linker and DIV S6 suggest that protein 14-3-3 is unlikely to influence the AAD's effects by direct interaction with the AADs molecule or the binding sites. Our results showed that 14-3-3 inhibition has different effects on different drugs, and different tendencies to promote or subdue the channel gating functions (i.e. activation, recovery, and SSI). This divergence further indicated that the 14-3-3 regulation of AADs effect is likely not through 14-3-3 directly binding with drug, masking or revealing the binding sites. Instead, it is likely linked to the role 14-3-3 plays in biophysical coupling of the sodium channel. 14-3-3 could also be involved through modulation of the sodium channel conformation in a steady state or changes in conformation during the channel gating. Thus, the DI-DII linker, due to the involvement of 14-3-3, could be another important site for the sodium channel's pharmaceutical effects due to its modulation of the biophysical coupling.

The results that difopein can diminish the use-dependent effect are particularly interesting as it is a direction that industry is looking for in drug development. Our findings suggest that a strategy targeting the specific inhibition of 14-3-3 action on the cardiac sodium channel could increase the efficacy of class I anti-arrhythmics. However, a broad inhibition of 14-3-3 is not a viable option in the clinical setting due to the promiscuous roles of 14-3-3 in human physiology. We believe that 14-3-3 has a fundamental role in cardiac electrophysiology and could be developed into a therapeutic target itself or shed light for expansion of novel therapeutics. Therefore, this

JPET Fast Forward. Published on December 2, 2022 as DOI: 10.1124/jpet.122.001407
This article has not been copyedited and formatted. The final version may differ from this version.

study provided new information about how 14-3-3 influences the Nav1.5 pharmaceutical responses, and built the foundation for novel therapeutic strategies targeting 14-3-3 as it relates to arrhythmias.

In conclusion, we demonstrated that inhibiting protein 14-3-3 could greatly influence the cardiac sodium channel's response to AADs, including altered AAD block on the peak current, biophysical kinetics, use- and dose-dependent block. Our observations reinforced the significance of $Na_v1.5$ coupling, and indicated that this channel characteristic needs to be considered carefully in the study of $Na_v1.5$-related therapeutics. It also highlighted the necessity of future studies to reveal more structural information regarding the $Na_v1.5$ coupling and interacting proteins and how it relates to the action of AADs.

Authorship Contributions

Participated in research design: Y Zheng, I Deschenes

Conducted experiments: Y Zheng

Performed data analysis: Y Zheng

Wrote or contributed to the writing of the manuscript: Y Zheng, I Deschenes

Reference

Abriel H (2010) Cardiac sodium channel Na(v)1.5 and interacting proteins: Physiology and pathophysiology. *J Mol Cell Cardiol* **48**:2-11.

Adsit GS, Vaidyanathan R, Galler CM, Kyle JW and Makielski JC (2013) Channelopathies from mutations in the cardiac sodium channel protein complex. *J Mol Cell Cardiol* **61**:34-43.

Allouis M, Le Bouffant F, Wilders R, Peroz D, Schott JJ, Noireaud J, Le Marec H, Merot J, Escande D and Baro I (2006) 14-3-3 is a regulator of the cardiac voltage-gated sodium channel Nav1.5. *Circ Res* **98**:1538-1546.

Clatot J, Hoshi M, Wan X, Liu H, Jain A, Shinlapawittayatorn K, Marionneau C, Ficker E, Ha T and Deschenes I (2017) Voltage-gated sodium channels assemble and gate as dimers. *Nat Commun* **8**:2077.

Clatot J, Zheng Y, Girardeau A, Liu H, Laurita KR, Marionneau C and Deschenes I (2018) Mutant voltage-gated Na(+) channels can exert a dominant negative effect through coupled gating. *Am J Physiol Heart Circ Physiol* **315**:H1250-H1257.

Cummins TR (2007) Setting up for the block: the mechanism underlying lidocaine's use-dependent inhibition of sodium channels. *J Physiol* **582**:11.

Fonseca DJ and Vaz da Silva MJ (2018) Cardiac channelopathies: The role of sodium channel mutations. *Rev Port Cardiol (Engl Ed)* **37**:179-199.

Fu DG (2015) Cardiac Arrhythmias: Diagnosis, Symptoms, and Treatments. *Cell Biochem Biophys* **73**:291-296.

Galleano I, Harms H, Choudhury K, Khoo K, Delemotte L and Pless SA (2021) Functional cross-talk between phosphorylation and disease-causing mutations in the cardiac sodium channel Nav1.5. *Proc Natl Acad Sci U S A* **118**.

Gavillet B, Rougier JS, Domenighetti AA, Behar R, Boixel C, Ruchat P, Lehr HA, Pedrazzini T and Abriel H (2006) Cardiac sodium channel Nav1.5 is regulated by a multiprotein complex composed of syntrophins and dystrophin. *Circ Res* **99**:407-414.

Heath BM, Cui Y, Worton S, Lawton B, Ward G, Ballini E, Doe CP, Ellis C, Patel BA and McMahon NC (2011) Translation of flecainide- and mexiletine-induced cardiac sodium channel inhibition and ventricular conduction slowing from nonclinical models to clinical. *J Pharmacol Toxicol Methods* **63**:258-268.

Hondeghem LM and Matsubara T (1988) Quinidine blocks cardiac sodium channels during opening and slow inactivation in guinea-pig papillary muscle. *Br J Pharmacol* **93**:311-318.

Huang Y, He Q, Yang M and Zhan L (2013) Antiarrhythmia drugs for cardiac arrest: a systemic review and meta-analysis. *Crit Care* **17**:R173.

Itoh H, Shimizu M, Takata S, Mabuchi H and Imoto K (2005) A novel missense mutation in the SCN5A gene associated with Brugada syndrome bidirectionally affecting blocking actions of antiarrhythmic drugs. *J Cardiovasc Electrophysiol* **16**:486-493.

Kecskemeti V (1991) Molecular action of class I antiarrhythmic drugs and clinical implications. *Pharmacol Res* **24**:131-142.

Kim YG, Oh SK, Choi HY and Choi JI (2021) Inherited arrhythmia syndrome predisposing to sudden cardiac death. *Korean J Intern Med* **36**:527-538.

Li T, Lu G, Chiang EY, Chernov-Rogan T, Grogan JL and Chen J (2017) High-throughput electrophysiological assays for voltage gated ion channels using SyncroPatch 768PE. *PLoS One* **12**:e0180154.

Li Z, Jin X, Wu T, Huang G, Wu K, Lei J, Pan X and Yan N (2021) Structural Basis for Pore Blockade of the Human Cardiac Sodium Channel Nav 1.5 by the Antiarrhythmic Drug Quinidine*. *Angew Chem Int Ed Engl* **60**:11474-11480.

Liu H, Atkins J and Kass RS (2003) Common molecular determinants of flecainide and lidocaine block of heart Na+ channels: evidence from experiments with neutral and quaternary flecainide analogues. *J Gen Physiol* **121**:199-214.

Masters SC and Fu H (2001) 14-3-3 proteins mediate an essential anti-apoptotic signal. *J Biol Chem* **276**:45193-45200.

Montnach J, Lorenzini M, Lesage A, Simon I, Nicolas S, Moreau E, Marionneau C, Baro I, De Waard M and Loussouarn G (2021) Computer modeling of whole-cell voltage-clamp analyses to delineate guidelines for good practice of manual and automated patch-clamp. *Sci Rep* **11**:3282.

Pless SA, Galpin JD, Frankel A and Ahern CA (2011) Molecular basis for class Ib anti-arrhythmic inhibition of cardiac sodium channels. *Nat Commun* **2**:351.

Pott C, Dechering DG, Muszynski A, Zellerhoff S, Bittner A, Wasmer K, Mönnig G and Eckardt L (2010) Class I Antiarrhythmic Drugs Mechanisms, Contraindications, and Current Indications. *Herzschrittmachertherapie + Elektrophysiologie* **21**:228-238.

Ragsdale DS, McPhee JC, Scheuer T and Catterall WA (1994) Molecular determinants of state-dependent block of Na+ channels by local anesthetics. *Science* **265**:1724-1728.

Ragsdale DS, McPhee JC, Scheuer T and Catterall WA (1996) Common molecular determinants of local anesthetic, antiarrhythmic, and anticonvulsant block of voltage-gated Na+ channels. *Proc Natl Acad Sci U S A* **93**:9270-9275.

Ramos E and O'Leary M E (2004) State-dependent trapping of flecainide in the cardiac sodium channel. *J Physiol* **560**:37-49.

Ruhlmann AH, Korner J, Hausmann R, Bebrivenski N, Neuhof C, Detro-Dassen S, Hautvast P, Benasolo CA, Meents J, Machtens JP, Schmalzing G and Lampert A (2020) Uncoupling sodium channel dimers restores the phenotype of a pain-linked Nav 1.7 channel mutation. *Br J Pharmacol* **177**:4481-4496.

Salata JJ and Wasserstrom JA (1988) Effects of quinidine on action potentials and ionic currents in isolated canine ventricular myocytes. *Circ Res* **62**:324-337.

Shenasa M, Shenasa M-A and Smith M (2020) Class I Antiarrhythmic Drugs: Na+ Channel Blockers, in pp 31-105, Springer International Publishing.

Shuraih M, Ai T, Vatta M, Sohma Y, Merkle EM, Taylor E, Li Z, Xi Y, Razavi M, Towbin JA and Cheng J (2007) A common SCN5A variant alters the responsiveness of human sodium channels to class I antiarrhythmic agents. *J Cardiovasc Electrophysiol* **18**:434-440.

Srinivasan NT and Schilling RJ (2018) Sudden Cardiac Death and Arrhythmias. *Arrhythm Electrophysiol Rev* **7**:111-117.

Starmer CF, Grant AO and Strauss HC (1984) Mechanisms of use-dependent block of sodium channels in excitable membranes by local anesthetics. *Biophys J* **46**:15-27.

Stevers LM, Sijbesma E, Botta M, MacKintosh C, Obsil T, Landrieu I, Cau Y, Wilson AJ, Karawajczyk A, Eickhoff J, Davis J, Hann M, O'Mahony G, Doveston RG, Brunsveld L and

Ottmann C (2018) Modulators of 14-3-3 Protein-Protein Interactions. *J Med Chem* **61**:3755-3778.

Sunami A, Fan Z, Sawanobori T and Hiraoka M (1993) Use-dependent block of Na+ currents by mexiletine at the single channel level in guinea-pig ventricular myocytes. *Br J Pharmacol* **110**:183-192.

Tan Z, Huang S, Mei K, Liu M, Ma J, Jiang Y, Zhu W, Yu P and Liu X (2021) The Prevalence and Associated Death of Ventricular Arrhythmia and Sudden Cardiac Death in Hospitalized Patients With COVID-19: A Systematic Review and Meta-Analysis. *Front Cardiovasc Med* **8**:795750.

Tikhonov DB and Zhorov BS (2017) Mechanism of sodium channel block by local anesthetics, antiarrhythmics, and anticonvulsants. *J Gen Physiol* **149**:465-481.

Wang B, Yang H, Liu YC, Jelinek T, Zhang L, Ruoslahti E and Fu H (1999) Isolation of high-affinity peptide antagonists of 14-3-3 proteins by phage display. *Biochemistry* **38**:12499-12504.

Wang Y, Mi J, Lu K, Lu Y and Wang K (2015) Comparison of Gating Properties and Use-Dependent Block of Nav1.5 and Nav1.7 Channels by Anti-Arrhythmics Mexiletine and Lidocaine. *PLoS One* **10**:e0128653.

Xiong H, Bai X, Quan Z, Yu D, Zhang H, Zhang C, Liang L, Yao Y, Yang Q, Wang Z, Wang L, Huang Y, Li H, Ren X, Tu X, Ke T, Xu C and Wang QK (2022) Mechanistic insights into the interaction of cardiac sodium channel Nav1.5 with MOG1 and a new molecular mechanism for Brugada syndrome. *Heart Rhythm* **19**:478-489.

Zheng Y, Wan X, Yang D, Ramirez-Navarro A, Liu H, Fu JD and Deschenes I (2021) A Heart Failure-Associated SCN5A Splice Variant Leads to a Reduction in Sodium Current Through Coupled-Gating With the Wild-Type Channel. *Front Physiol* **12**:661429.

Zhu Y, Kyle JW and Lee PJ (2006) Flecainide sensitivity of a Na channel long QT mutation shows an open-channel blocking mechanism for use-dependent block. *Am J Physiol Heart Circ Physiol* **291**:H29-37.

JPET Fast Forward. Published on December 2, 2022 as DOI: 10.1124/jpet.122.001407
This article has not been copyedited and formatted. The final version may differ from this version.

Figure Legends

Figure 1. 14-3-3 inhibition increased $Na_v1.5$ block by quinidine. The sodium currents were recorded in HEK293 cells by high throughput automated patch-clamp in whole-cell configuration. 14-3-3 was inhibited by difopein (difo). A. Representative current traces for each conditions. B. Current-voltage (I/V) relationship. Voltage protocol is included. C. Quantification of the sodium current block by all four AADs. Statistical analysis was done by two-tailed paired t-test.

Figure 2. 14-3-3 inhibition shifted the conductance curves under the influence of AADs. The voltage-dependent conductance curves for quinidine (A), lidocaine (B), mexiletine (C), and flecainide (D) were derived from the I/V curves as described in "Material and Method". Quinidine (A) and flecainide (D) did not exert significant effect on the activation, while lidocaine (B) and mexiletine (C) shifted the activation curves toward depolarizing voltages. Compared with the drug only effects, 14-3-3 inhibition shifted all the activation curves toward hyperpolarizing voltages.

Figure 3. 14-3-3 impact on steady-state inactivation (SSI) curves of the sodium current under the influence of AADs. The sodium currents were recorded from HEK293 cells in whole-cell configuration. SSI curves for quinidine (A), lidocaine (B), mexiletine (C), and flecainide (D) and the voltage protocol are shown in the figure. 14-3-3 inhibition removed the quinidine effect on SSI, and shifted the SSI of lidocaine (B) and flecainide (D) toward hyperpolarizing voltages.

JPET Fast Forward. Published on December 2, 2022 as DOI: 10.1124/jpet.122.001407
This article has not been copyedited and formatted. The final version may differ from this version.

Figure 4. Impact of 14-3-3 on sodium channel's recovery from inactivation under the influence of AADs. The sodium currents were recorded from HEK293 cells in whole-cell configuration. Recovery curves for quinidine (A), lidocaine (B), mexiletine (C), and flecainide (D) and the voltage protocol are shown in the figure. Lidocaine (B) and mexiletine (C) slowed the channel recovery from inactivation without the involvement of 14-3-3, while 14-3-3 inhibition further slowed the channel recovery for the quinidine (A) and flecainide (D).

Figure 5. 14-3-3 impacts quinidine's dose-dependent block. The dose-dependency of quinidine (A), lidocaine (B), mexiletine (C), and flecainide (D) are shown in the figure. 14-3-3 inhibition lowered the IC50 of quinidine (A).

Figure 6. Impact of 14-3-3 inhibition on the use-dependent block at 1Hz stimulation. A train of 50 pulses was applied to the channel. The holding potential was -120mV and the test pulses were -30mV for 10ms. 14-3-3 inhibition had not impact on the use-dependent block of the four drugs tested at 1Hz.

Figure 7. Impact of 14-3-3 inhibition on the use-dependent block at 5Hz stimulation. A train of 30 pulses was applied to the HEK293 cells. 14-3-3 inhibition diminished use-dependent block of lidocaine (B), mexiletine (C), and flecainide (D) but not quinidine (A).

Figure 8. Impact of 14-3-3 inhibition on the use-dependent block at 10Hz stimulation. A train of 30 pulses was applied to the HEK293 cells. 14-3-3 inhibition diminished use-dependent block of lidocaine (B) and mexiletine (C) without affecting quinidine (A) and flecainide (D).

JPET Fast Forward. Published on December 2, 2022 as DOI: 10.1124/jpet.122.001407
This article has not been copyedited and formatted. The final version may differ from this version.

Figure 9. Summary of the 14-3-3 effects on the use-dependent block of A. quinidine, B. lidocaine, C. mexiletine, and D. flecainide.

JPET Fast Forward. Published on December 2, 2022 as DOI: 10.1124/jpet.122.001407
This article has not been copyedited and formatted. The final version may differ from this version.

Table 1. $Na_v1.5$ Biophysical Parameters

Parameters / Conditions	Activation $V_{1/2}$ (mV)	n	SSI $V_{1/2}$ (mV)	n	A_{rec}	i_{rec}	τ_{rec} (ms)	n
Control	-50.50 ±0.11	33	-98.06 ±0.12	44	0.96 ±0.0018	0.98 ±0.0085	17.47 ±1.32	35
Quinidine	-49.32 ±0.08	29	-93.89 ±0.42*	35	0.94 ±0.0029*	0.91 ±0.018*	15.05 ±1.08	26
Quinidine_difopein	-52.77 ±0.14**	31	-99.21 ±0.38^{+}	30	0.94 ±0.0081*	0.81 ±0.024**	28.53 ±3.22**	17
Lidocaine	-45.34 ±0.14*	36	-95.57 ±0.24*	46	0.79 ±0.0044*	0.77 ±0.014*	16.71 ±1.24	29
Lidocaine_difopein	-49.68 ±0.11^{+}	31	-102.96 ±0.26^{+}	32	0.77 ±0.0057*	0.71 ±0.013**	25.54 ±2.39**	15
Mexiletine	-45.08 ±0.19*	31	-96.11 ±0.27	33	0.76 ±0.0060*	0.70 ±0.014*	16.18 ±1.35	18
Mexiletine_difopein	-48.39 ±0.14^{+}	28	-98.82 ±0.25	28	0.77 ±0.0073*	0.66 ±0.027**	19.18 ±2.85	15
Flecainide	-49.08 ±0.23	24	-96.36 ±0.41	12	0.92 ±0.023*	0.89 ±0.03*	12.11 ±5.24	4
Flecainide_difopein	-52.27±0.08^{+}	29	-102.81 ±0.38**	24	0.91 ±0.022*	0.80 ±0.049	20.34 ±8.33	5

*: significantly different from control ($p<0.05$)

$^{+}$: significantly different from the corresponding drug group($p<0.05$)

**: significantly different from control and the corresponding drug group ($p<0.05$)

JPET Fast Forward. Published on December 2, 2022 as DOI: 10.1124/jpet.122.001407
This article has not been copyedited and formatted. The final version may differ from this version.

Footnotes

No author has an actual or perceived conflict of interest with the contents of this article.

This work was supported by the National Institutes of Health [Grant R01HL094450, R01HL096962 to ID].

Figure 1

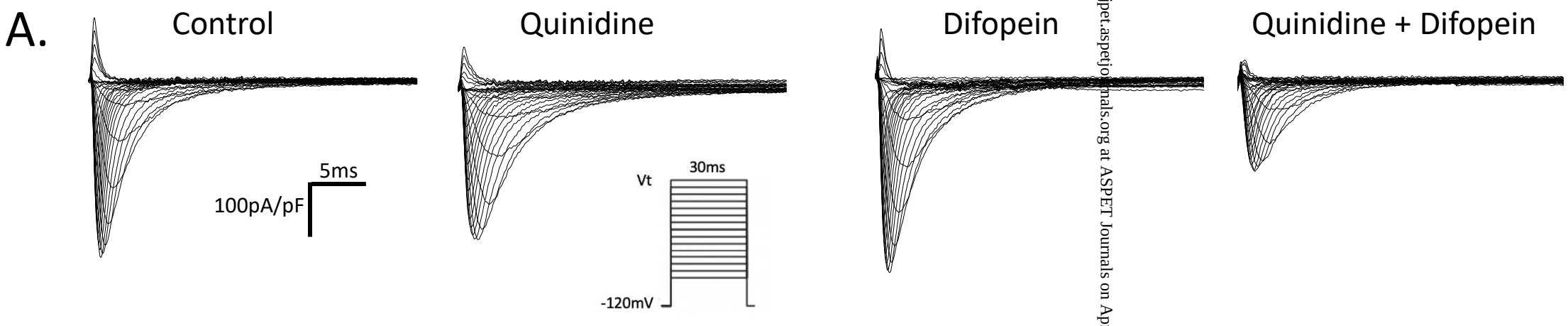

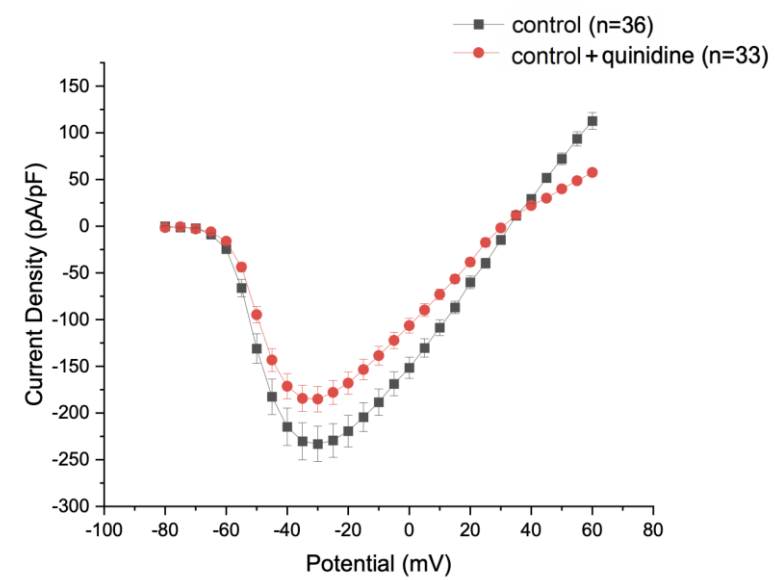

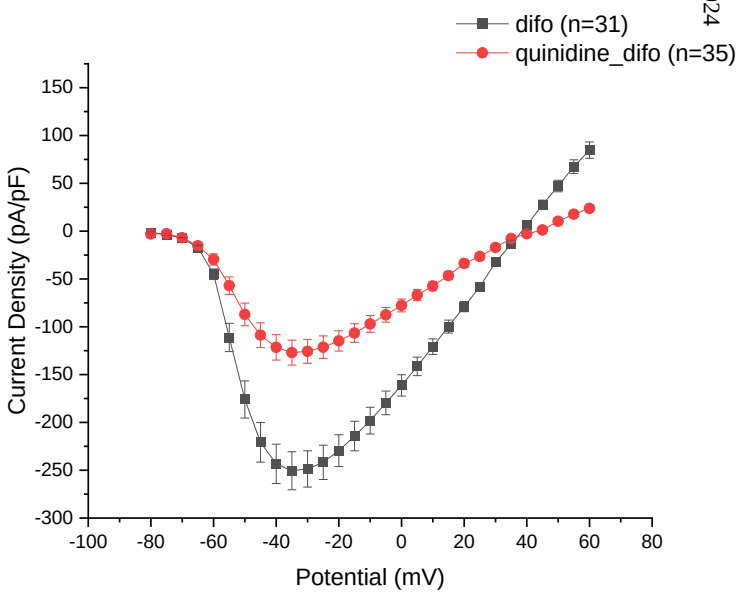

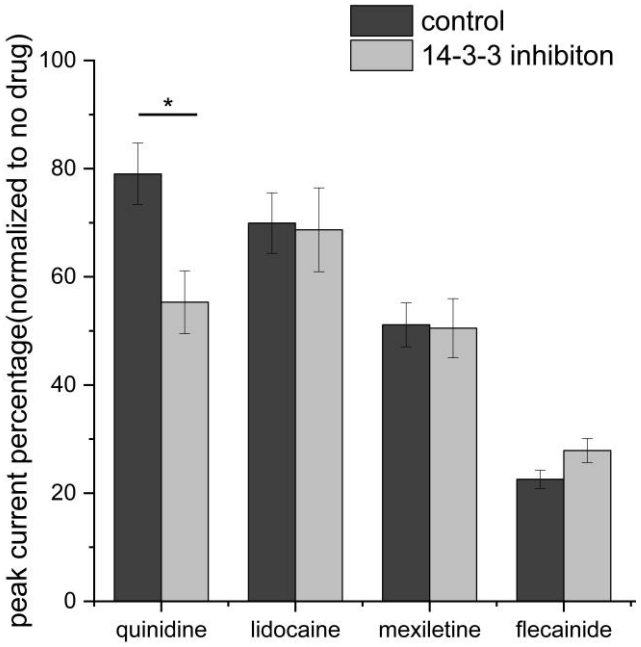

Figure 2

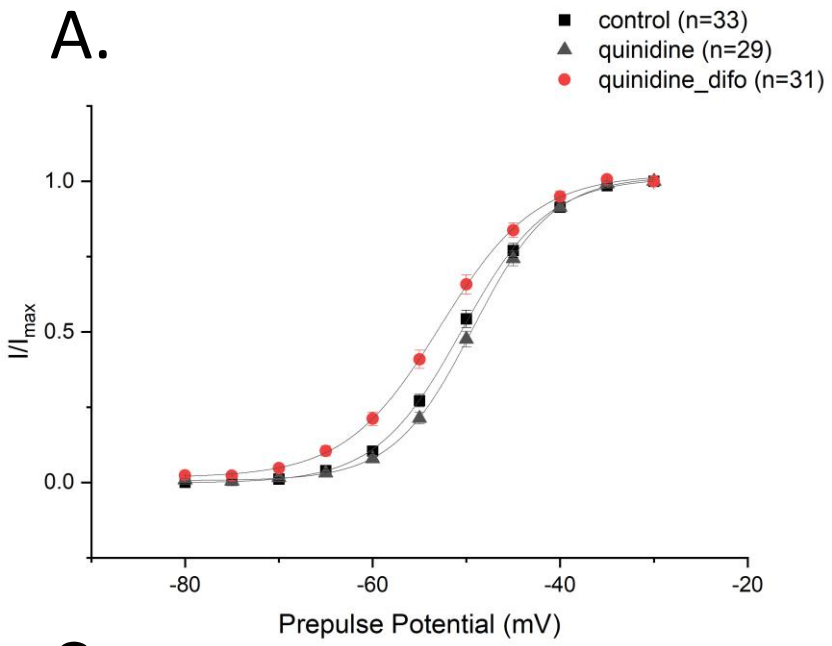

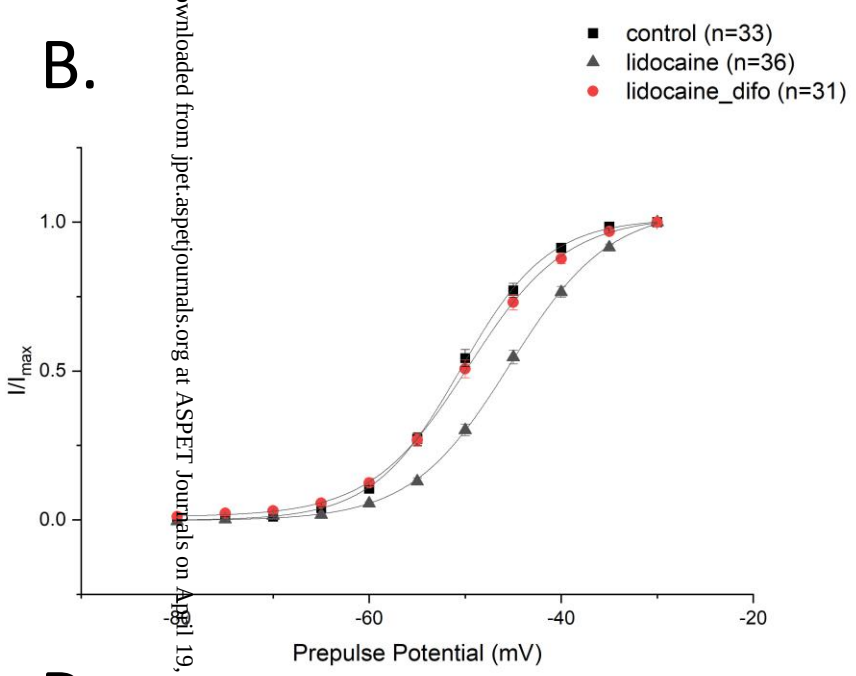

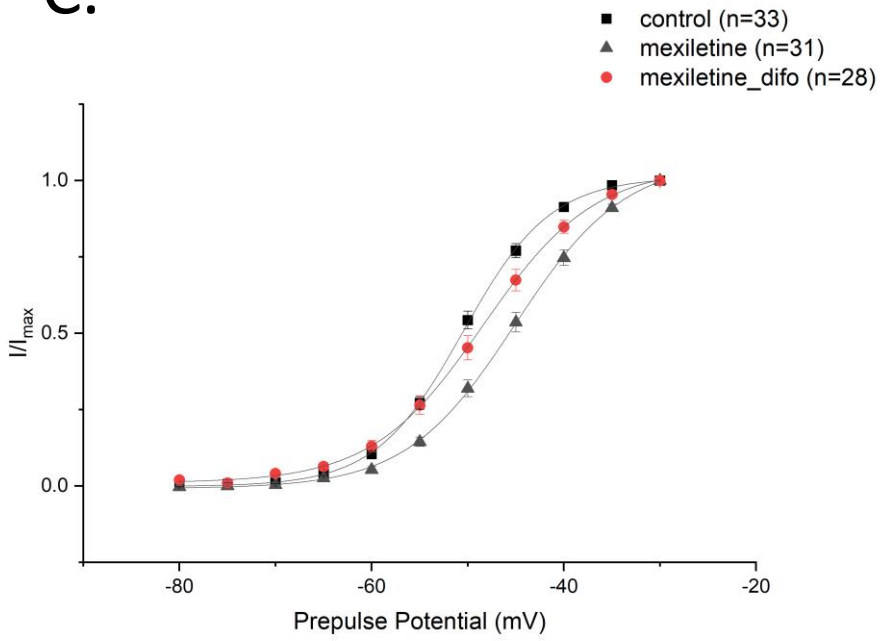

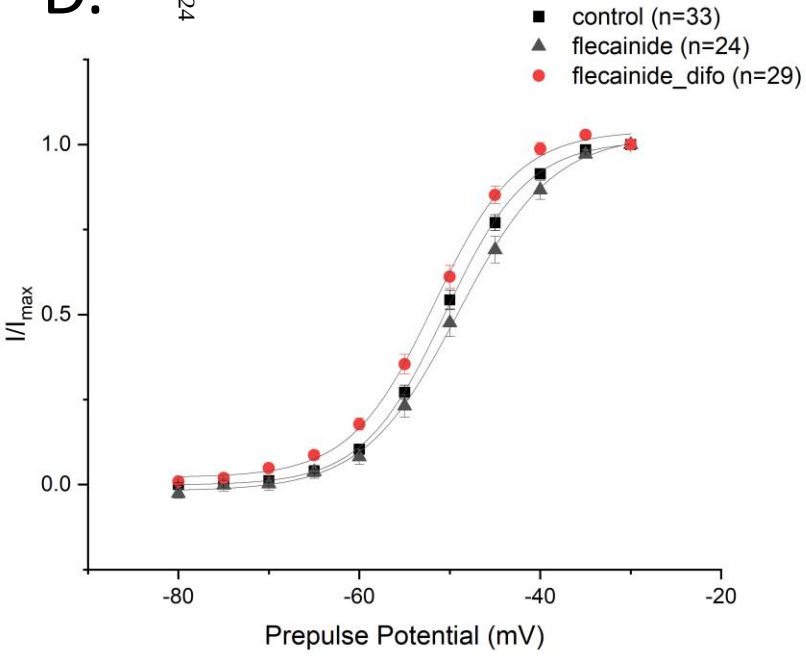

Figure 3

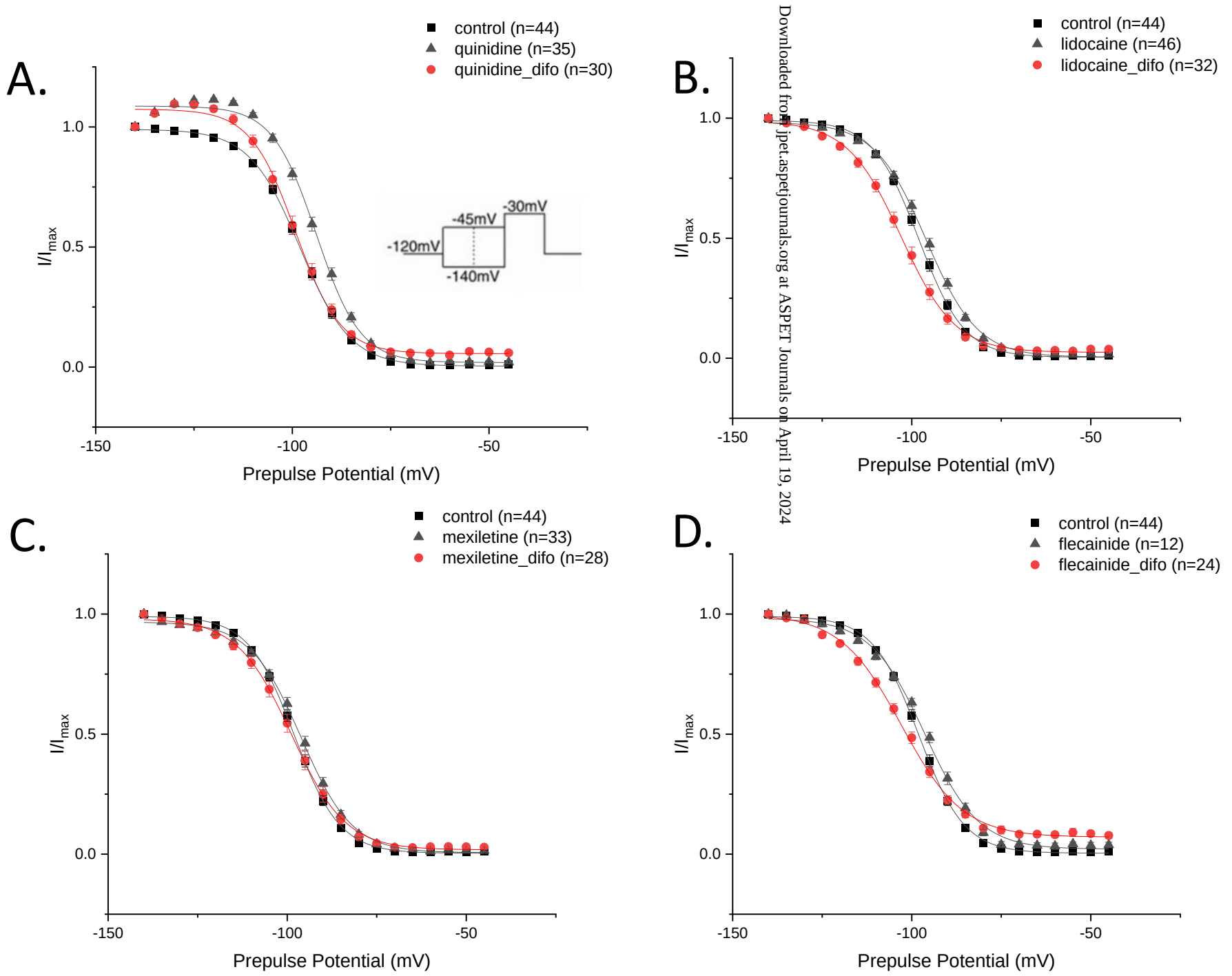

Figure 4

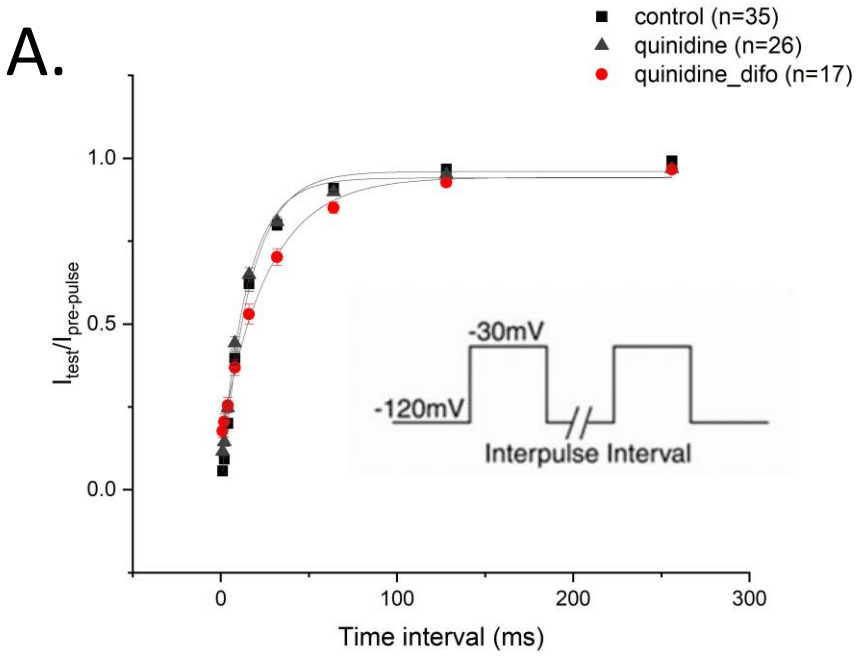

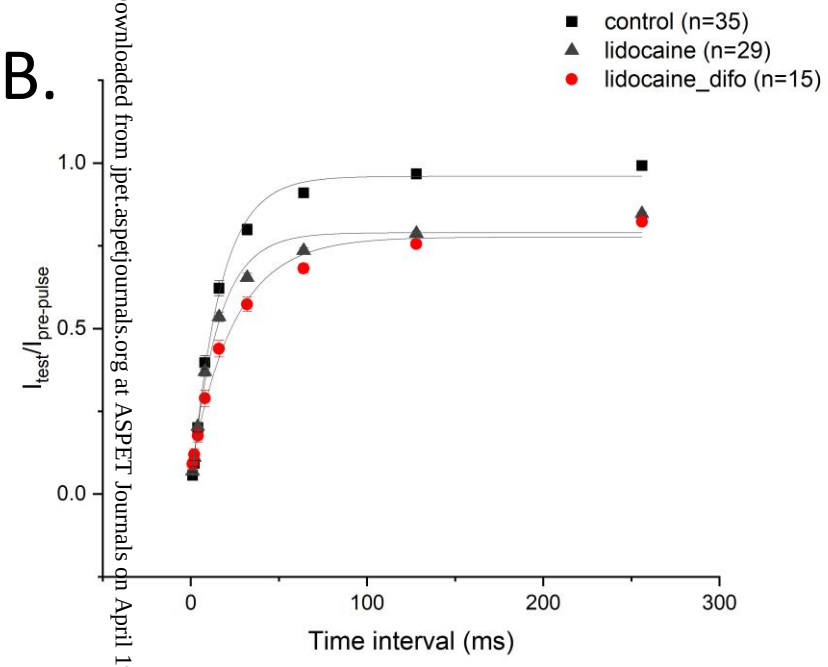

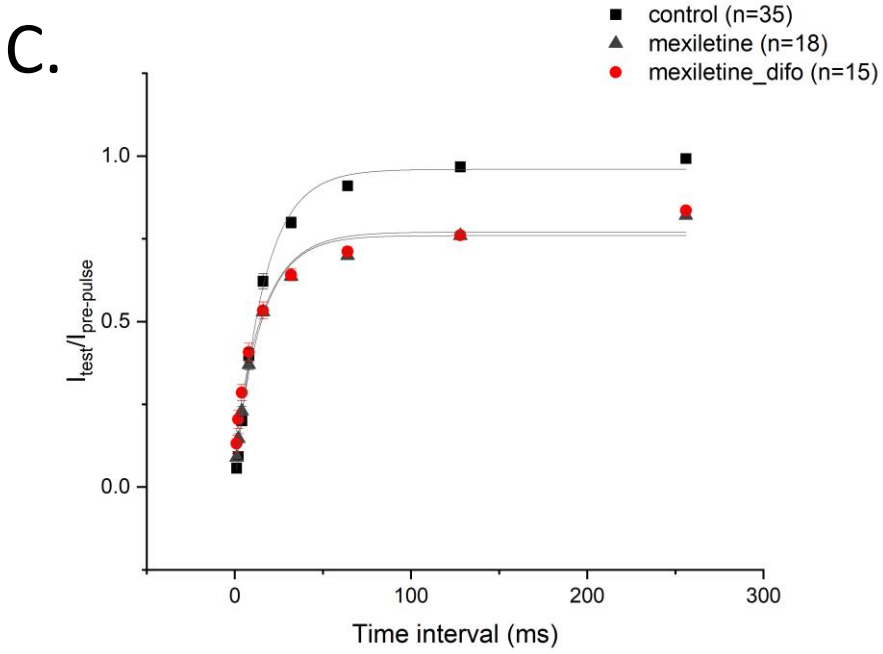

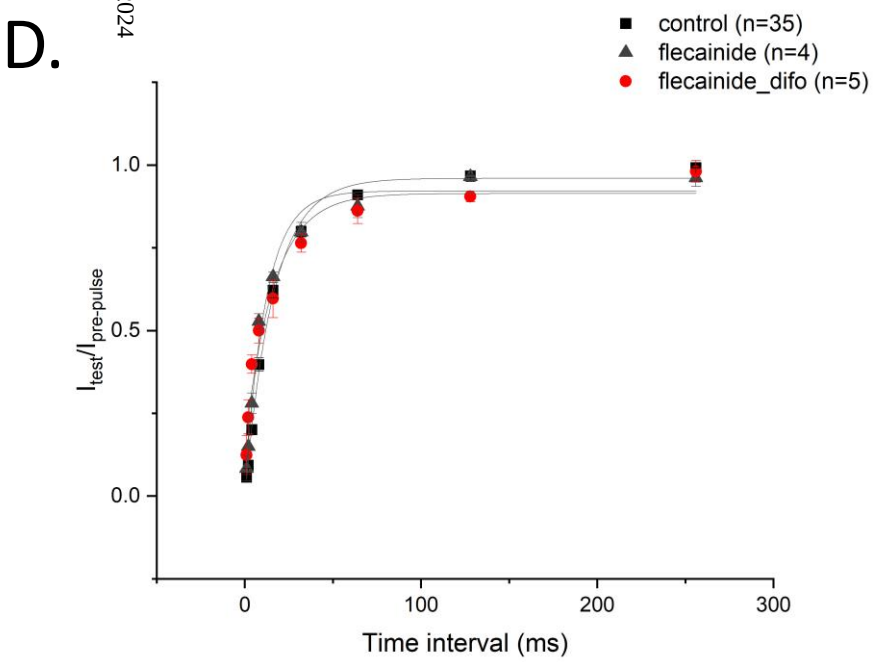

Figure 5

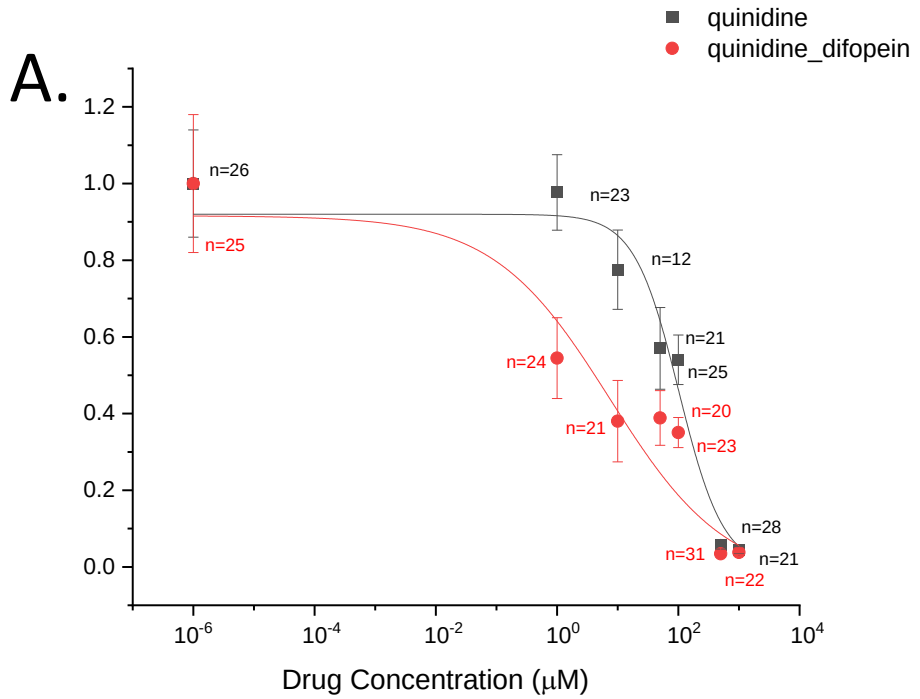

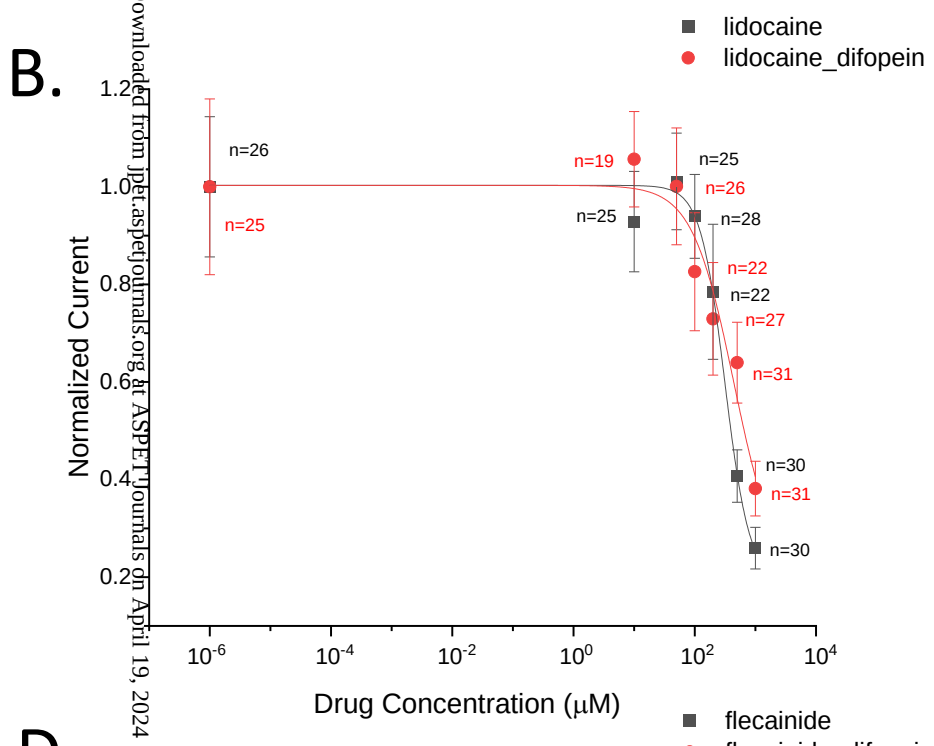

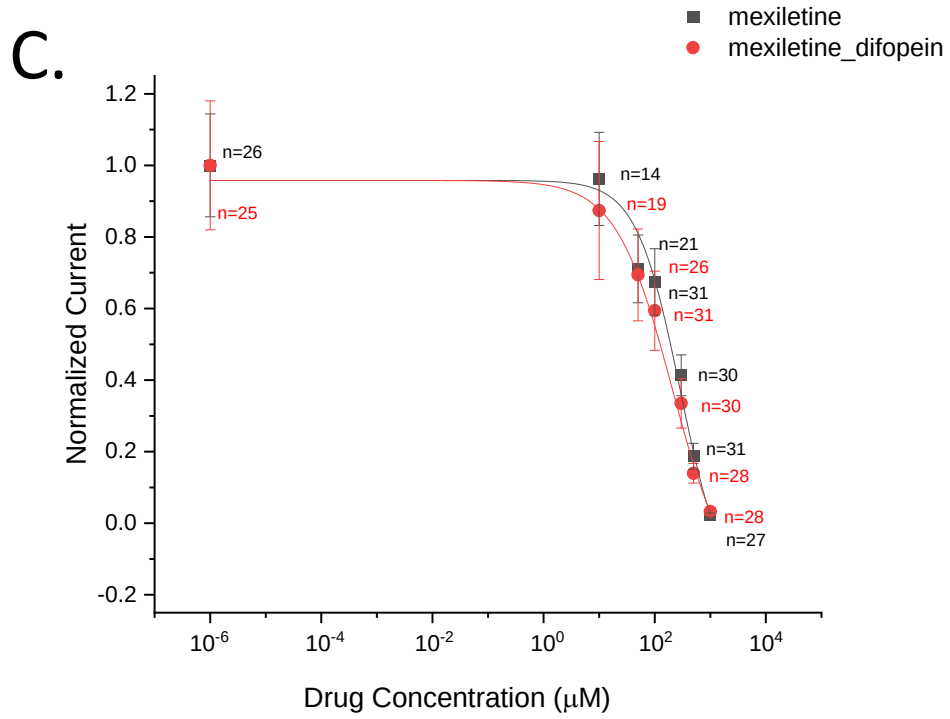

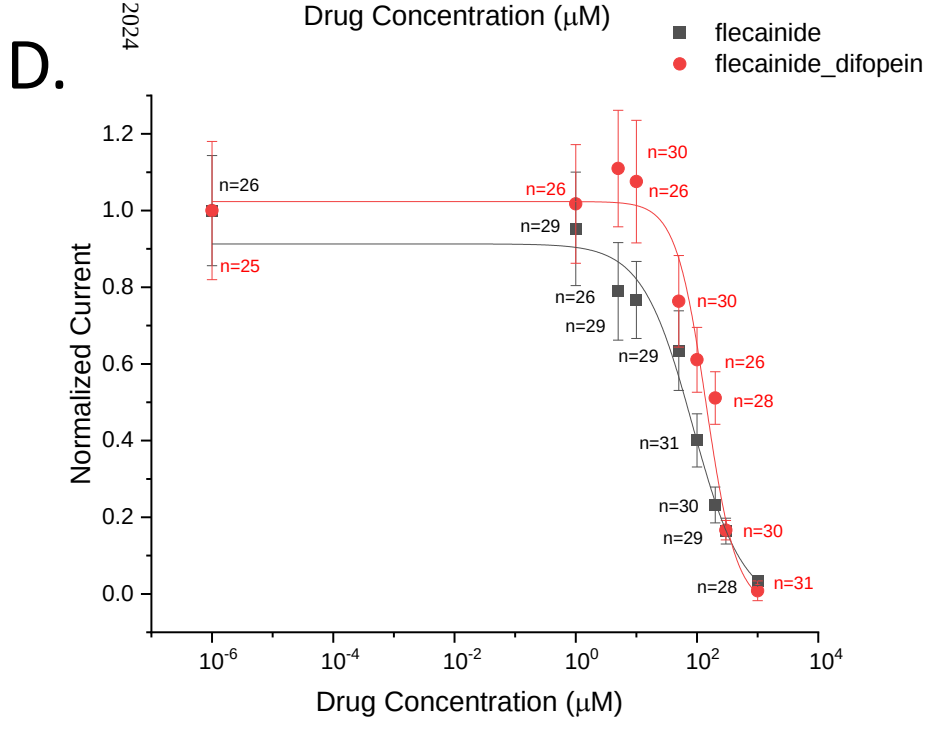

Figure 6

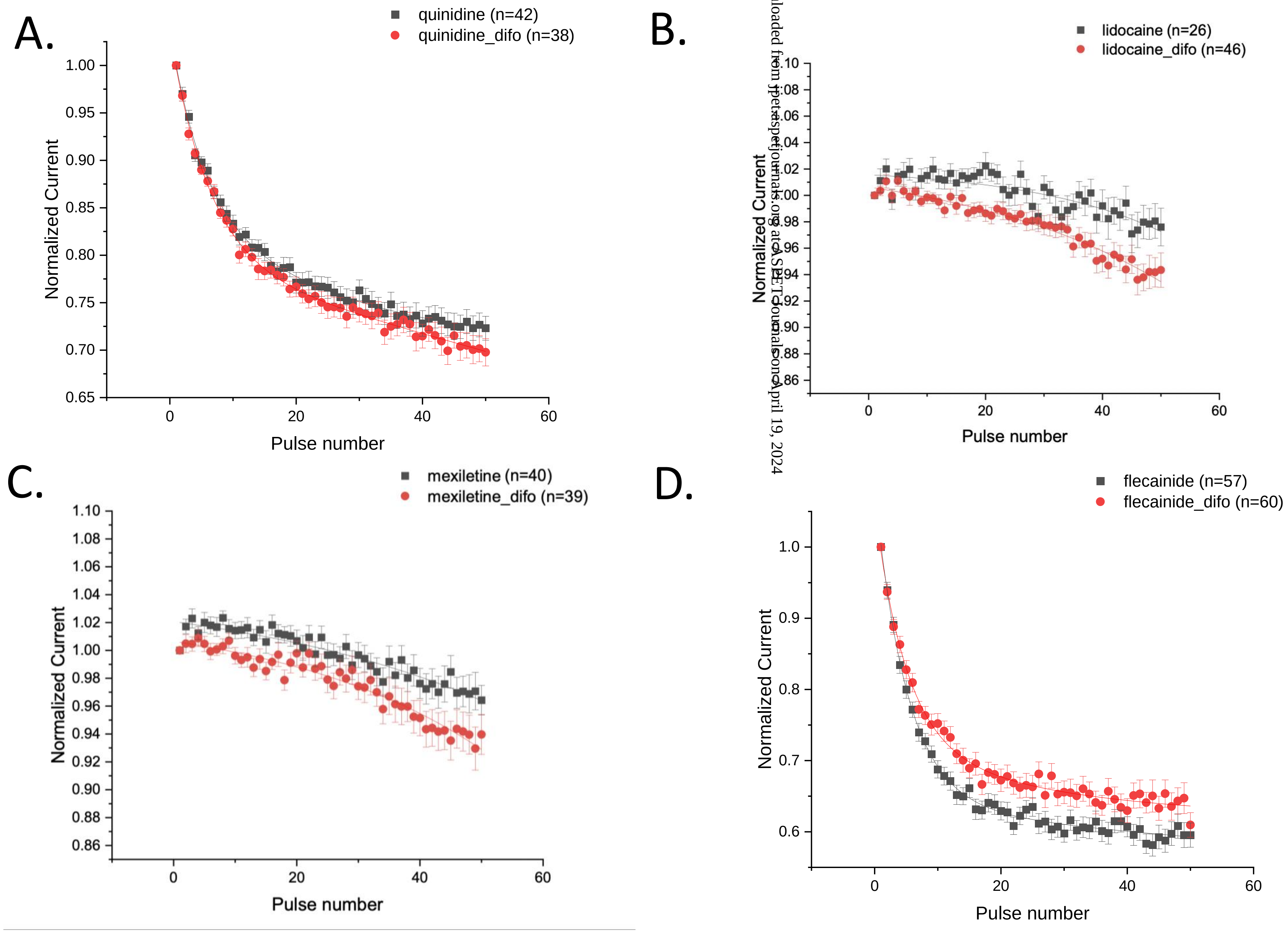

Figure 7

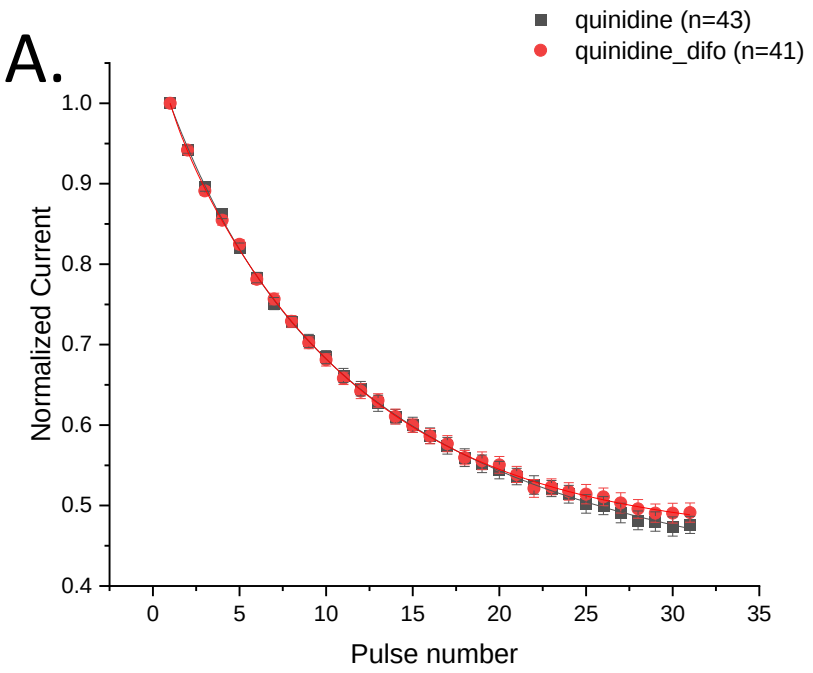

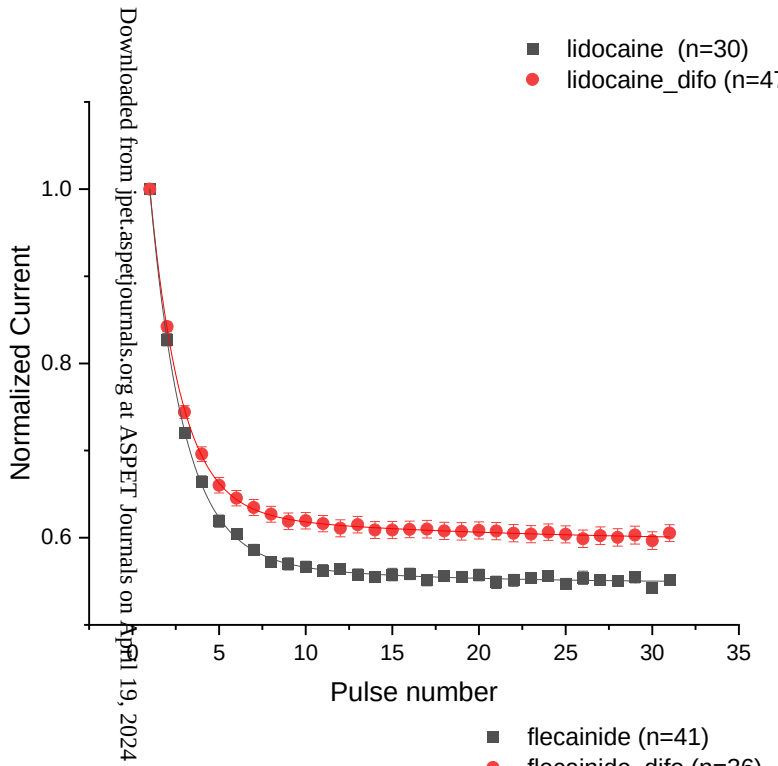

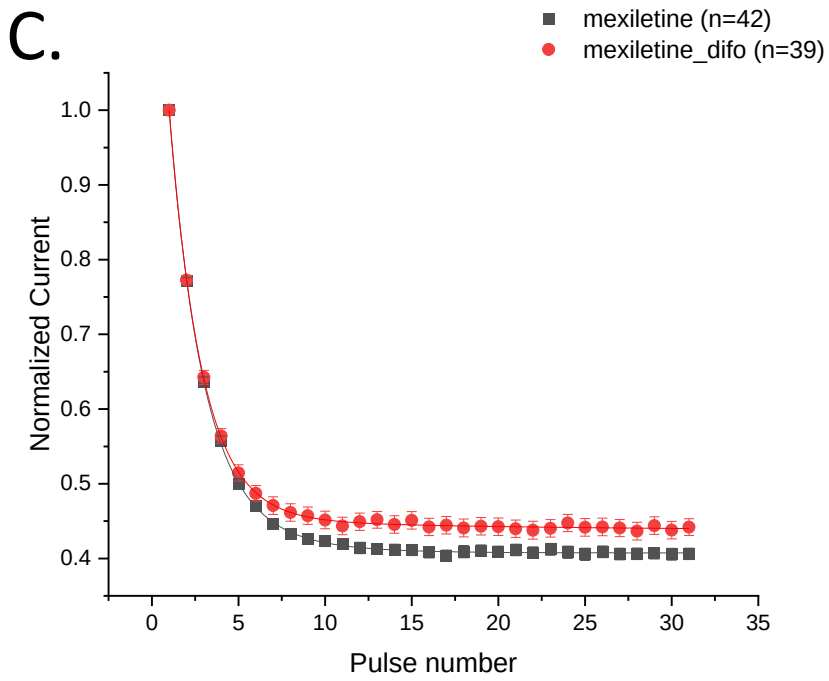

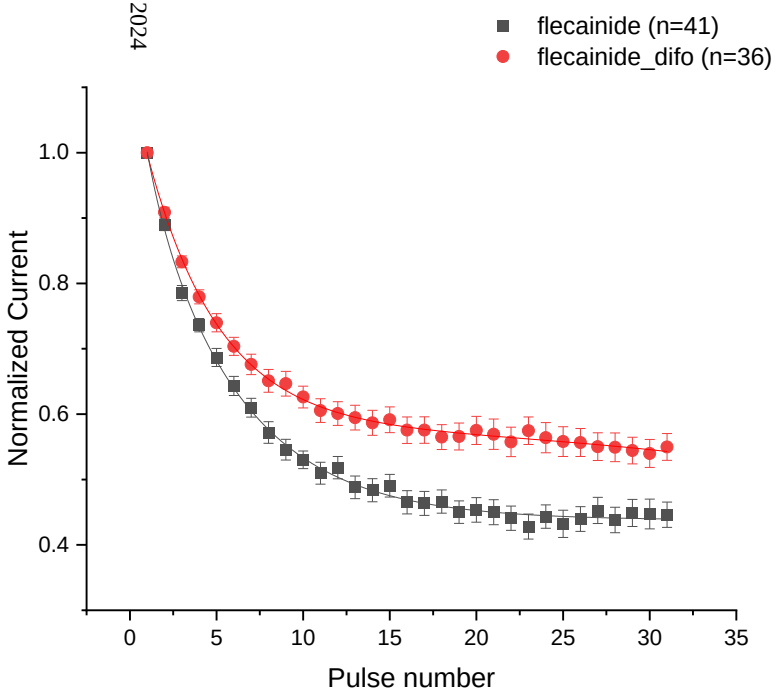

Figure 8

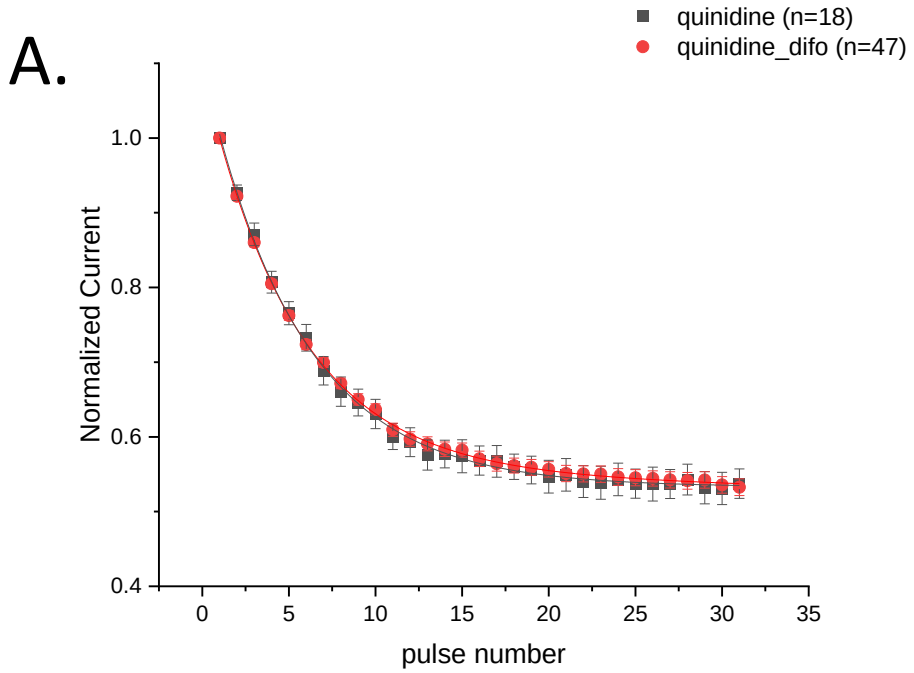

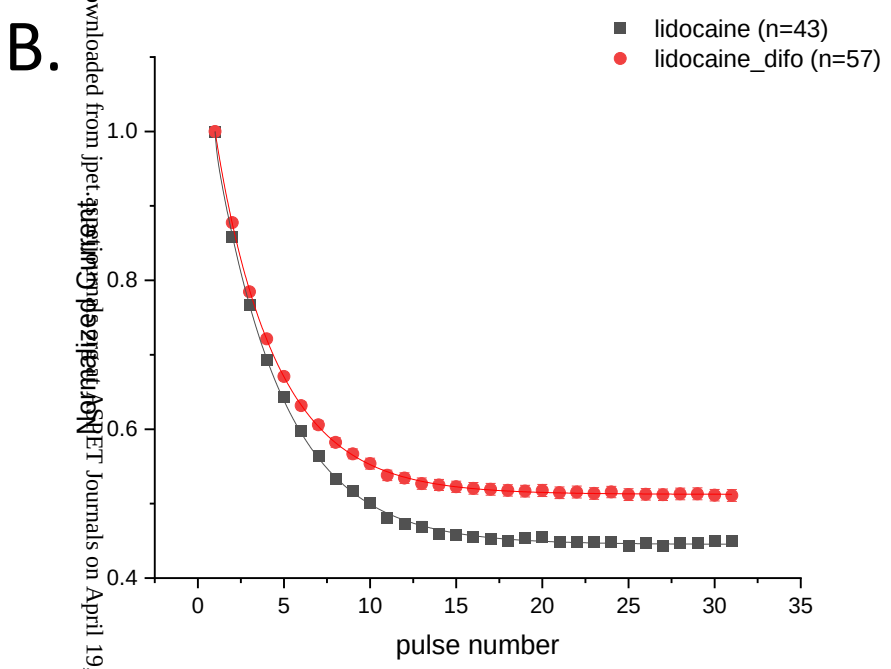

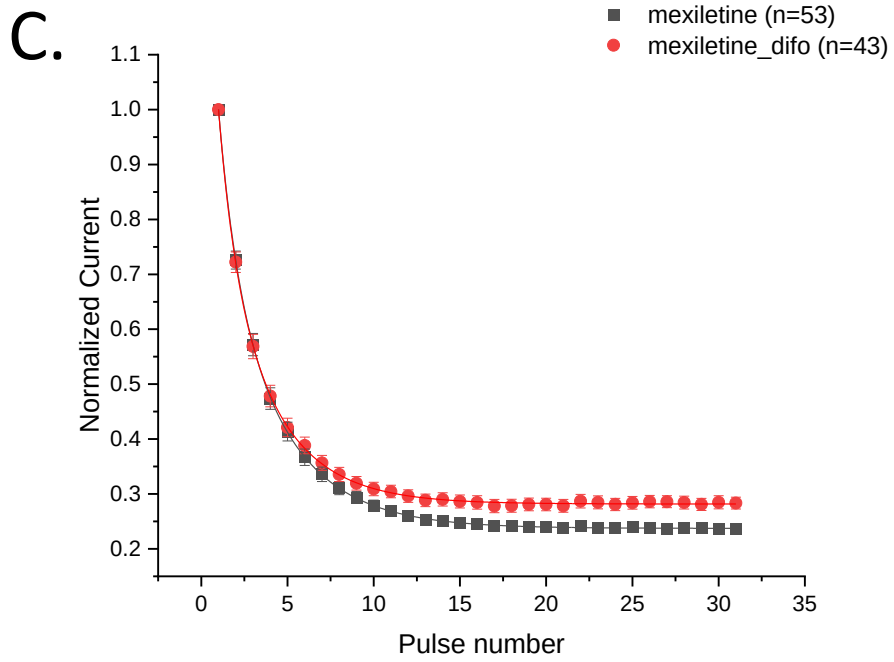

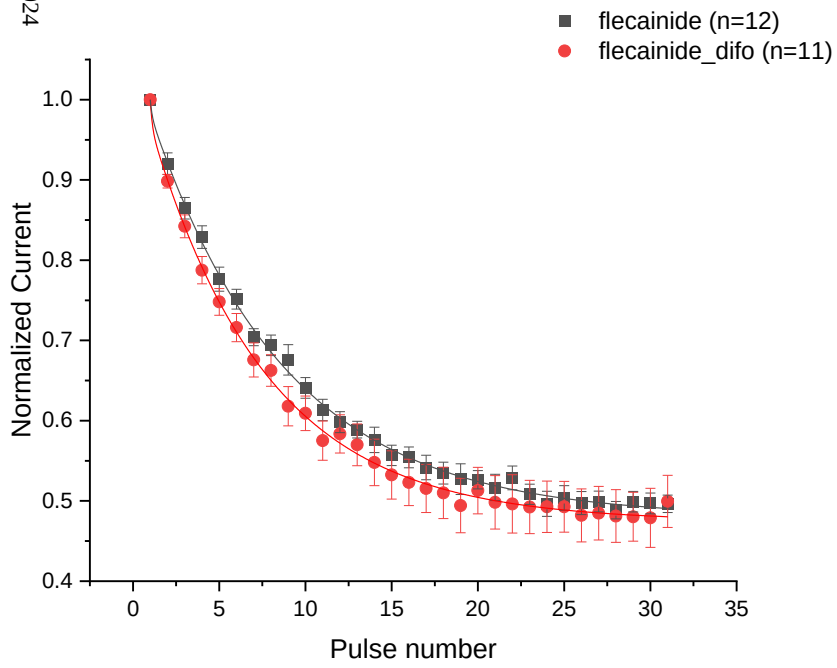

Figure 9

A.

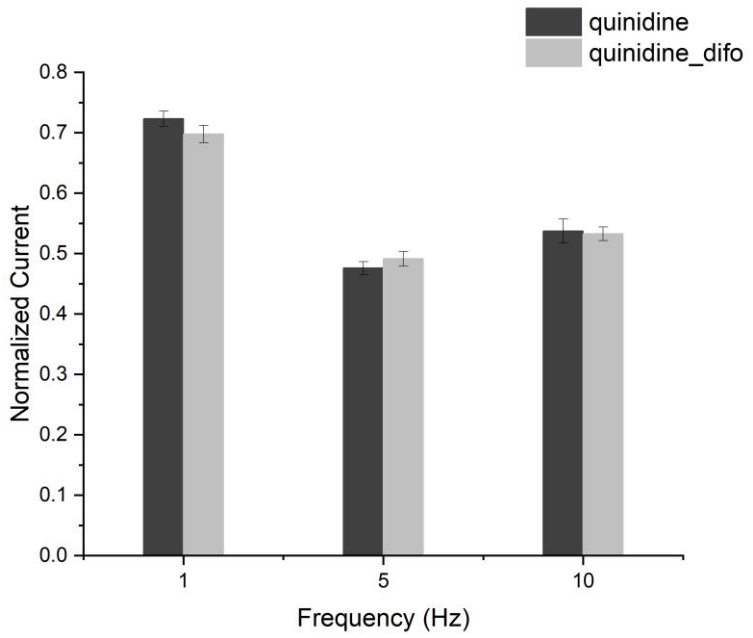

B.

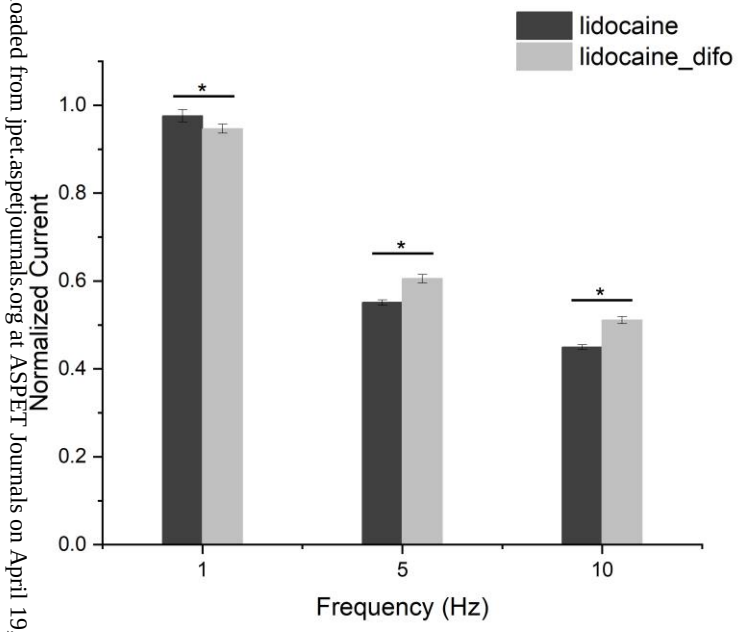

C.

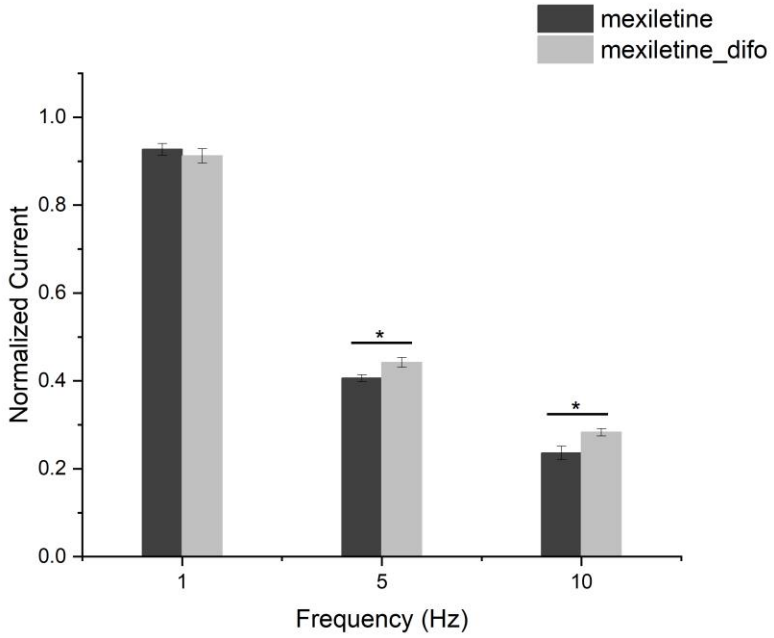

D.